Actin at cell-cell junctions is composed of two dynamic and functional populations

Juankun Zhang[1,*], Martha Betson[1,*,‡], Jennifer Erasmus[1], Kostas Zeikos[1], Maryse Bailly[2], Louise P. Cramer[3] and Vania M. M. Braga[1,§]

[1]Molecular and Cellular Medicine, Faculty of Life Sciences, Imperial College London, Sir Alexander Fleming Building, London, SW7 2AZ, UK
[2]Institute of Ophthalmology, University College London, 11-43 Bath Street, London, EC1V 9EL, UK
[3]Laboratory for Molecular Cell Biology and Department of Biology, University College London, Gower Street, London, WC1E 6BT, UK
*These authors contributed equally to this work
‡Present address: MGH Cancer Center and Harvard Medical School, Chalestown, MA, USA
§Author for correspondence (e-mail: v.braga@imperial.ac.uk)

Accepted 15 August 2005
Journal of Cell Science 118, 5549-5562 Published by The Company of Biologists 2005
doi:10.1242/jcs.02639

Summary

The ability of epithelial cells to polarize requires cell-cell adhesion mediated by cadherin receptors. During cell-cell contact, the mechanism via which a flat, spread cell shape is changed into a tall, cuboidal epithelial morphology is not known. We found that cadherin-dependent adhesion modulates actin dynamics by triggering changes in actin organization both locally at junctions and within the rest of the cell. Upon induction of cell-cell contacts, two spatial actin populations are distinguishable: junctional actin and peripheral thin bundles. With time, the relative position of these two populations changes and becomes indistinguishable to form a cortical actin ring that is characteristic of mature, fully polarized epithelial cells. Junctional actin and thin actin bundles differ in their actin dynamics and mechanism of formation, and interestingly, have distinct roles during epithelial polarization. Whereas junctional actin stabilizes clustered cadherin receptors at cell-cell contacts, contraction of peripheral actin bundle is essential for an increase in the maximum height at the lateral domain during polarization (cuboidal morphology). Thus, both junctional actin and thin bundles are necessary, and cooperate with each other to generate a polarized epithelial morphology.

Key words: Microfilaments, Keratinocytes, Actin bundles, Cadherins, Cell-cell contact

Supplementary material available online at
http://jcs.biologists.org/cgi/content/full/118/23/5549/DC1

Introduction

Epithelial cells are morphologically polarized: they are characterized by distinct membrane domains, a cuboidal cell shape and strong attachment to neighbouring cells and underlying basement membrane (Nelson, 2003). As cell shape is intrinsically related to epithelial function and actin cytoskeleton organization, great effort has been put into understanding the actin reorganization that occurs during morphological differentiation. Herein, polarization is defined as the process by which epithelial cells remodel the cytoskeleton to acquire the tall, cuboidal cell shape.

In epithelia, actin bundles are present as a thick circumferential ring around each cell, aligned with the cell borders (Owaribe et al., 1981; Yonemura et al., 1995; Zamansky et al., 1991). In addition to the circumferential organization, a less abundant population of actin bundles also appear to terminate at sites of cell-cell contacts as assessed by electron microscopy and immunofluorescence (Green et al., 1987; Sanger et al., 1983; Vasioukhin et al., 2000; Yonemura et al., 1995; Zamansky et al., 1991).

Surprisingly, there are currently no mechanistic insights into how, in flat epithelial cells prior to polarization, the cytoskeleton is reorganized into the typical circumferential ring organization for mature cells as described above. So far, the knowledge on specific epithelial actin structures and their formation has been limited when compared to information available in other cell systems (motile cell types). As the maintenance of epithelial morphology is a key factor for homeostasis and function, it is important to identify actin cytoskeletal structures required for polarization and their mechanism of formation. Once specific actin activities and structures are defined, the identification of their regulatory mechanisms and relevant proteins will be more focused.

What is known about the morphological polarization process? During polarization, a series of steps are triggered: (1) formation of new cell-cell contacts, (2) stabilization of these new contacts, (3) junction maturation and (4) acquisition of a cuboidal cell morphology. The time frame in which these steps occur varies according to the cell type and culture conditions, e.g. cell confluence (McNeill et al., 1993; Vasioukhin et al., 2000). Up to now, only the early events related to junction assembly have been studied in detail (steps 1 and 2 above).

In the first step, i.e. the formation of new cell-cell contacts, it is well established that adhesion mediated by cadherin receptors is essential (Yap et al., 1997). Cadherins provide calcium-dependent cell-cell adhesion and interact indirectly with the actin cytoskeleton (Yap et al., 1997). In the presence of calcium ions, cells probe each other in a series of transient, weak contacts, mediated by homophilic interaction of cadherin

Journal of Cell Science

receptors ('zippering' model). These weak contacts are followed by clustering of cadherins into structures called 'puncta' (Adams et al., 1996; McNeill et al., 1993).

Puncta appear within minutes of the initial cell-cell contact as discrete dots at contacting membranes, and actin recruitment to puncta occurs concomitantly or shortly after. Actin recruitment is predicted to restrict the mobility of clustered cadherin receptors at the plane of the membrane and to reinforce adhesion, facilitating the progression from transient to stable contacts (step 2) (Adams et al., 1998; Adams et al., 1996). Actin-mediated stabilization of newly formed contacts is manifested as a continuous line of cadherin/actin staining at cell-cell borders (step 2) as opposed to the punctate pattern observed earlier. At this point, considerable interdigitation of neighbouring membranes is seen in some cell types (Vaezi et al., 2002; Vasioukhin et al., 2000).

Once cell-cell contacts are stabilized, the junction maturation process takes place (step 3 – time frame not known). The actin cytoskeleton in cells with newly formed junctions (steps 1 and 2) must be remodelled in some way, as yet unknown, to produce the circumferential actin ring coincident with the junctions (Owaribe et al., 1981). Finally, full acquisition of polarity takes place: a cuboidal morphology develops, with a tall lateral domain and neighbouring cells compact towards each other (step 4, time frame unknown).

Thus, epithelial morphological polarization and actin reorganization are complex processes. Clearly, there is a large reorganization of microfilaments, particularly during the junction maturation and full polarization processes (steps 3 and 4). However, the spatial and temporal changes and the precise mechanisms involved to complete polarization are not well understood. For example, how further actin recruitment to stable junctions is coordinated with actin filament reorganization to form the circumferential actin ring is not clear (step 3). In addition, very little is known about which actin reorganization process is required for the development of a tall, cuboidal cell shape (step 4).

To begin to address some of these questions, we focused on precise actin dynamic steps required for complete morphological polarization. We tested potential mechanisms for the formation of actin structures that are well understood in other model cell systems, but surprisingly have not yet been investigated during epithelial polarization. Typically, the formation of diverse actin structures involves actin assembly, activity of myosin family proteins (particularly actin bundle contractility) or both. Furthermore, a number of distinct actin assembly mechanisms can be distinguished by differences in dynamics and supply of actin monomer 'fuel' to power assembly (reviewed by Pollard et al., 2000). For instance, actin may assemble at the barbed end or at both the barbed and pointed end, depending on the cell type (Littlefield et al., 2001). Moreover, the supply of monomers for actin assembly in motile cells may come from previously stored or recently disassembled pools, depending on whether the cell is polarized and migrating (Cramer et al., 2002; Cramer, 1999).

During epithelial polarization, new actin assembly is required at puncta (step 1), but the role of assembly in all subsequent steps is unclear. Conversely, myosin function during the early steps is not known, but it does play a role in cell compaction (step 4) (Adams et al., 1998; Collins and Fleming, 1995). Myosin II and other myosin family members are localized at cell-cell junctions (Krendel et al., 1999; Owaribe et al., 1981; Philip and Nachmias, 1985; Stoffler et al., 1998), and may participate in the expansion of cell membranes as adhesive contacts are formed (step 1) (Adams et al., 1998; Gloushankova et al., 1998; Yonemura et al., 1995). Other potential additional roles for myosin II contractility, such as in formation of the circumferential actin ring (step 3) and acquisition of a cuboidal cell shape (step 4), have yet to be formally demonstrated.

In this work, we used normal human keratinocytes, a well established model for studying the formation of cadherin-dependent cell-cell contacts and epithelial polarization (Braga, 2000). To exclude any potential contribution of cell migration to the actin reorganization events, only confluent keratinocyte cultures were used to induce cell-cell contacts. Using this model, we focus on three important questions that have not been addressed in the literature. (1) What is the detailed organization of actin during the stabilization and maturation steps? (2) What is the mechanism of formation and dynamics of distinct actin structure during epithelial polarization? (3) What is the relative importance of these different actin populations for junction assembly and acquisition of a tall, cuboidal cell shape?

We found that, upon initial cell-cell contact, two spatial actin populations are observed: a continuous line of actin at junctions (junctional actin) and peripheral thin bundles. These spatial populations can be further distinguished by their actin dynamics and mechanism of formation. After cell-cell contacts are stabilized, thin bundles appear to coalesce towards the junctional actin population to form a straight line of the thicker, continuous F-actin bundle, reminiscent of the circumferential ring observed in mature epithelia (mature junctional actin). Equally important, this process is accompanied by an increase in myosin-dependent contractility and the acquisition of a polarized cell shape in keratinocytes.

Materials and Methods

Cell culture

Normal human keratinocytes (strains Kb, AEK and Sa, passages 3-7) were cultured on a mitomycin C-treated monolayer of 3T3 fibroblasts at 37°C with 5% CO_2, as previously described (Hodivala and Watt, 1994). To induce cell-cell contacts, confluent cultures grown in low calcium medium were transferred to standard calcium medium for different amounts of time (Hodivala and Watt, 1994).

Antibodies and immunofluorescence

Primary antibodies used were anti-actin (C4, mouse monoclonal; MP Biomedicals, London, UK), anti-E-cadherin (HECD-1 mouse monoclonal [a gift from M. Takeichi (Shimoyama et al., 1989)] and ECCD-2 rat monoclonal (Hirai et al., 1989). Anti-phosphorylated myosin light chain (S19, mouse monoclonal) was a kind gift from M. Matsuda (Osaka University, Japan). Secondary antibodies were purchased from Jackson ImmunoResearch Laboratories (Stratech Scientific, Luton, UK). Fluorescein isothiocyanate (FITC)-phalloidin was purchased from Sigma. Labelled actin (FITC- or Alexa Fluor 568-G-actin) and DNAse1 (Alexa Fluor 488-DNAse1) were purchased from Molecular Probes (Paisley, UK).

Unless otherwise stated, cells were fixed, permeabilized and stained as described previously (Braga et al., 1997). To visualize labelled actin at cell-cell contacts after microinjection and in latrunculin B

experiments, cells were fixed in 3% paraformaldehyde containing 0.5% Triton X-100 for 10 minutes at room temperature. Staining using C4 anti-actin antibodies was performed as described previously (Cramer, 1999). To visualize labelling of actin bundles, cells were pre-extracted with detergent before fixation in 3% paraformaldehyde (Braga et al., 1995).

Confocal images were obtained with a Leica DM IRBE microscope, containing a krypton-argon laser and TCS NT software. Cells were also viewed using an Olympus Provis AX70 microscope and digital images were collected with Spot RT monochrome cooled charge-coupled (CCD) camera and software (Diagnostic Instruments) or with a KAF 1400 CCD camera (Roper Scientific) on a Nikon microscope using Metamorph software (Cramer et al., 2002). Images were processed using Adobe Photoshop, Metamorph and Volocity Software.

Drug treatment

Confluent keratinocytes grown in low calcium medium, which does not induce cell-cell contacts, were transferred to standard calcium medium containing different drugs or vehicle control. Latrunculin B (Calbiochem) was carefully titrated (0.2 μM) to obtain disruption of the actin cytoskeleton without producing actin aggregates in the cytoplasm or cell retraction. In other experiments, latex beads (15 μm, PolySciences) coated with anti-cadherin antibodies or BSA (Braga et al., 1997) were incubated for 15-20 minutes with keratinocytes in the appropriate medium (low or standard calcium medium).

Jasplakinolide is a toxin that has two distinct activities: it stabilizes actin filaments (thereby preventing actin disassembly) and, more slowly, induces actin polymerization (Bubb et al., 1994; Cramer, 1999). To separate these two activities the jasplakinolide concentration was carefully titrated as described previously (Cramer, 1999). Keratinocytes were treated with 0.01 μM jasplakinolide (Molecular Probes; see supplementary material Fig. S1) for 60 minutes or with 0.5 μM for shorter incubations (5 or 15 minutes), which did not induce actin aggregates. The same results were obtained after treatment with 1 μM (data not shown).

Inhibition of myosin contractility was achieved by treatment with blebbistatin, a drug that blocks myosin II ATPase activity (Merck) (Straight et al., 2003). Cells were incubated for 1 hour with blebbistatin titrated to 50 μM. In addition, Y27632 (25 μM, gift from A. Yoshimura) or ML9 (10 μM, Calbiochem) were used.

Incorporation of labelled G-actin

Microinjection was performed essentially as described previously (Braga et al., 1997). Confluent patches of keratinocytes cultured in low calcium medium were injected with either FITC or Alexa Fluor 568-G-actin (Molecular Probes) at a pipette concentration of 3 mg/ml. Immediately after microinjection, cells were transferred to standard calcium medium for various periods of time before fixation.

Live cells were permeabilized as described previously (Chan et al., 2000). Keratinocytes grown in low calcium medium were switched into standard calcium medium for 0, 5, 30 and 60 minutes. Cells were then incubated for 2 minutes in polymerization buffer [Alexa Fluor 568-actin (0.45 μM), 138 mM KCl, 10 mM PIPES pH 6.9, 0.1 mM ATP, 3 mM EGTA, 4 mM $MgCl_2$, 1% BSA and 0.025% saponin] with or without 2 μM cytochalasin B (Sigma). No difference in actin incorporation was seen when higher concentrations of saponin were used. For visualization of actin bundles, pEGFP-β-actin (2 μg) was transfected into confluent keratinocytes cultured in low calcium medium using Fugene 6 (Roche). After overnight incubation, keratinocytes were transferred to standard calcium medium for 1 hour to induce cell-cell contacts.

Analyses of G- and F-actin pools

G- and F-actin pools were analysed biochemically or by immunofluorescence. G- and F-actin pools were isolated from keratinocytes with newly formed cell-cell junctions essentially as described previously (Cramer et al., 2002), but using CSK buffer for extraction of G-actin pool (Braga et al., 1995). SDS-PAGE was performed on equal amounts of protein (BCA Kit, Pierce) and the gels were stained with Coomassie Blue. There was not much change in the total amount of actin during the time course (data not shown). Purified actin from rabbit muscle (kind gift from L. Machesky) was used as a reference.

G-actin was detected by immunofluorescence after staining with DNAse1 at 5 μg/ml, and cells were co-stained with phalloidin to quantify both actin pools in the same area (Cramer et al., 2002). Confocal Z-series were collected (1 μm thick) using the same settings for all time points; controls were performed to ensure there was no bleed through between the two channels. A maximum confocal projection was used for quantification of G- and F-actin (whole field or at the junctional actin region; see quantification below).

Quantification

To quantify the observed pattern of F-actin organization during new contact assembly, we classified the organization of thin bundles according to their precise position relative to the interface between neighbouring cells, into four different categories (see Fig. 1 legend). Images were taken at the focal plane where F-actin was apparent at cell-cell contacts. At different time points the number of cells showing each pattern was counted and expressed as a percentage of the population.

Quantification using immunofluorescence images was performed using the Leica Confocal Software. Actin dynamics were quantified from images obtained after microinjection of labelled actin. Because of variation in the amount of microinjected actin in different cells, the fluorescence intensity at bundles or junctional actin was divided by the background fluorescence for each measurement made. This ratio was plotted as fold increase over time. The best fit line was obtained to detect the rate of actin incorporation into thin bundles ($y=0.095x+1.032$), and junctional actin (neighbouring injected cells, $y=0.186x+1.100$). Quantification of latrunculin experiments were performed counting as positive cells that contain either junctional actin or any linear filaments (thin bundles remnants) at the cell periphery. Values were expressed as percentage of the total number of cells present in the micrograph.

The increase in P-MLC levels during induction of cell-cell contacts was quantified in two different ways. First, the overall increase was measured from western blots of keratinocyte lysates probed with anti P-MLC. Values were normalized by the amount of actin present in the same lysates and expressed relative to the P-MLC levels found in cells maintained in low calcium medium. Second, the sub-cellular increase in P-MLC levels was determined from confocal images by measuring the fluorescence intensity at thin bundles or the cell body.

The lateral domain height was measured by counting the number of confocal sections (0.3 μm thick) in which a linear staining for E-cadherin was observed at cell-cell contacts induced for 1 hour. Actin staining was used to determine the number of sections from the top (apex) to the base of the cell. The height of the lateral domain was calculated by multiplying the numbers of sections positive for E-cadherin staining by 0.3 μm (Z-step). Values were expressed relative to control untreated keratinocytes, assuming the height of the lateral domain in control cells as 100%.

G- and F-actin pools were quantified globally (biochemically and by immunofluorescence, whole optic field) or specifically at cell-cell contact areas (by immunofluorescence). When G- and F-actin were quantified at cell-cell contacts, only images at 0 and 15 minutes were used, as at this stage there is clear separation between junctional actin and thin bundles. At time zero, areas of close apposition of neighbouring membranes were chosen. Quantification of G- and F-

actin pools was expressed as a percentage of the total amount of actin at each time point.

Gels and X-ray films of different exposures of were scanned (Arcus 1200, AGFA) and relevant bands were quantified using Scion or TotalLab software (Nonlinear Dynamics, Mortsel, Belgium). Statistical analysis was performed using Student's *t*-test.

Results

Actin is organized into two spatial populations during induction of cell-cell contacts

In keratinocytes grown without cell-cell adhesion, thin actin bundles are already formed in a loose, broad band around the cell periphery (Low Ca^{2+}, Fig. 1A) (Zamansky et al., 1991). In the absence of contacts, cadherin receptors are diffusely expressed at the cell surface and in the cytoplasm (see also Fig. 2A) (Braga et al., 1995). As reported before, at early time points after junction initiation, F-actin is localized to cell-cell adhesion sites, coincident with cadherin receptors in two related staining patterns (Adams et al., 1998; Adams et al., 1996). These patterns are: (1) actin dots associated with initial cadherin puncta (within 2-4 minutes after contact initiation), and (2) more closely spaced actin dots aligned with cadherin receptors that tend to appear as a wavy, thin punctate line (Adams et al., 1998; Adams et al., 1996).

We observed both patterns after new cell-cell contact formation: the punctate actin pattern and the wavy, thin punctate line (Fig. 1A, 15 minutes Std. Ca^{2+}, upper and lower arrowhead, respectively). We define them together as junctional actin. We surmise that this temporal transition in the two staining patterns for junctional actin represent continued clustering of cadherin receptors and also actin association with other transmembrane proteins localized at cell-cell contacts. Separate from junctional actin we describe a new, distinct spatial and organizational population of actin, thin actin bundles. These bundles are in the same focal plane as junctional actin, but clearly flanking junctional actin (arrows, Std. Ca^{2+}, Fig. 1A). Thus, at early time points, two distinct actin populations can be separated by both position and by actin organization (see diagram in Fig. 1A). Moreover, these two populations can also be distinguished at the molecular level, according to cytoskeletal proteins that localize to each population (supplementary material Fig. S2).

Thin actin bundles observed after initiation of contacts seem similar to the looser array of bundles detected prior to cell-cell contact formation, except for one key difference, in that after initiation they appear more tightly packed (Fig. 1A). Furthermore, with

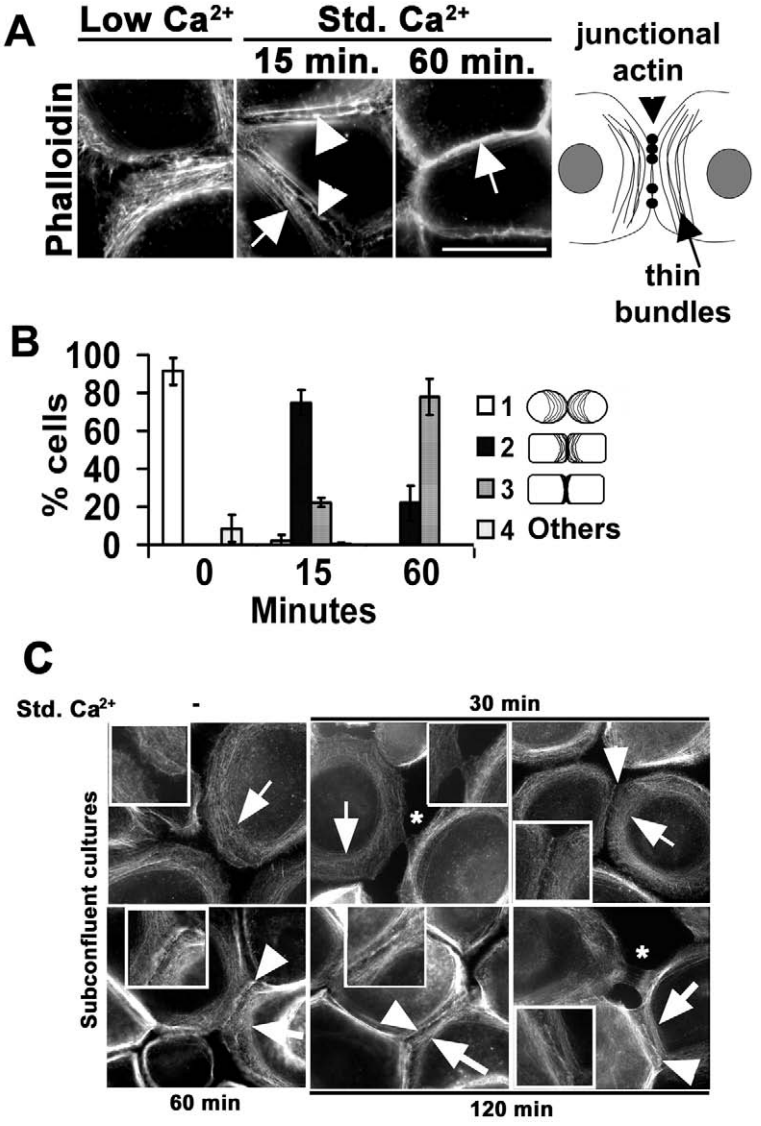

Fig. 1. Spatial distribution of actin populations during induction of cell-cell contacts. (A) Keratinocytes grown in low calcium medium (Low Ca^{2+}), which does not induce cell-cell contacts, were induced to form cadherin-dependent cell-cell adhesion (standard calcium medium, Std. Ca^{2+}). After junction formation, two actin populations can be distinguished on the basis of their location: one is present as a wavy, punctate line at junctions (junctional actin, arrowheads); the second population is a tighter array of thin bundles in the cytoplasm, flanking the junctional-actin population (arrow). By 60 minutes, the two populations are less readily distinguished (mature junctional actin). Bar, 50 μm. (B) Percentage of keratinocytes classified into four different categories according to the spatial organization of thin bundles following junction formation. Categories observed: (1) a wide, loose band of actin filaments, and no F-actin at cell-cell borders; (2) F-actin at junctions is visible (junctional actin) and the band of filaments localizes closer to cell-cell contacts; (3) junctional actin is more intense; filaments are more tightly bundled in a narrower region proximal to junctions or indistinguishable from F-actin at cell-cell contacts; (4) other phenotypes (less than 5-10% of total). Results are the average of two independent experiments, in which 200 cells were scored per time point in each experiment. (C) Following induction of cell-cell contacts in sub-confluent keratinocytes, cytoskeletal changes show a delayed formation of junctional actin and reorganization of thin bundles. For example, thin bundles are not coincident with junctional actin after 120 minutes of junction formation. Additional actin structures are also seen before junctional actin is properly stabilized (i.e. kissing structures, inset 30 minutes). Presumably these structures participate in the migration of two neighbouring cells towards each other as they are not readily observed in confluent cultures.

increased time after cell-cell contact formation (15-60 minutes), there seems to be further tighter packing of thin actin bundles such that the array of bundles becomes narrower and more closely positioned to junctional actin (Fig. 1B). By 60 minutes, junctional actin and thin actin bundles could not be distinguished in about 80% of cells (varies between 60-85% depending on keratinocyte strain and confluence; Fig. 1B). As this organization appears similar to that of actin at mature junctions in keratinocytes (Braga et al., 1995; Hodivala and Watt, 1994), we define it as mature junctional actin (60 minutes, Fig. 1A).

In a separate set of experiments, cell-cell junctions were induced in sub-confluent keratinocytes to test whether our results are applicable to cell-cell adhesion in general (Fig. 1C). In areas of similar sub-confluence, junctional actin formation was only initiated after 30 minutes of new cell-cell contact formation and progressive reorganization of bundles towards junctions was clearly still occurring by 2 hours. In addition, as reported before (Vasioukhin et al., 2000), in sub-confluent keratinocytes kissing structures (asterisks, Fig. 1C) were seen prior to the formation of junctional actin (arrowhead, Fig. 1C), suggesting that these structures extend to form continuous junctional actin. Thus, the sequential order of events is similar in confluent and sub-confluent cells, arguing that actin reorganization occurs via similar processes. One exception is that the formation of coincident junctional actin and thin bundles (seen by 1 hour in confluent keratinocytes) is severely delayed in sub-confluent cells because of a requirement for keratinocytes to move towards each other and initiate kissing structures (data not shown).

The two spatial populations of actin have distinct dynamics

The dynamics of junctional actin and thin bundles were evaluated in two ways: actin incorporation, and sensitivity to latrunculin (Fig. 2). In keratinocytes, within 20 minutes of induction of new contacts, incorporation of labelled actin monomers is detected at cell-cell contacts; this event is inhibited if cadherin adhesion is blocked (Braga et al., 1997). However, the incorporation of labelled actin monomers into thin bundles and their dynamics have not yet been evaluated in epithelial cells.

When keratinocytes were maintained in the absence of cell-cell contacts, there was little incorporation of labelled actin at cell-cell boundaries or into actin bundles, suggesting extremely slow dynamics (Low Ca^{2+}, Fig. 2B). As reported for other epithelial cell types, labelled actin recruitment to keratinocyte cell-cell contacts occurred rapidly ($t_{1/2}$=3 minutes) at sites where cadherin receptors localized and increased with time (arrowhead Fig. 2A, and data not shown) (Adams et al., 1998; Adams et al., 1996; McNeill et al., 1993). By contrast, incorporation of fluorescent actin monomers into thin bundles occurred more slowly ($t_{1/2}$=12 minutes; arrow Fig. 2B, and data not shown). Quantification of the above results revealed that the rate of actin incorporation at thin bundles (slope of graph 0.095) was slower than determined for junctional actin (slope of graph 0.186, Fig. 1C; see Materials and Methods for details). These data suggest that junctional actin is more dynamic than thin bundles.

As a second approach, differences in dynamics in the two actin populations were addressed by sensitivity to latrunculin B (Fig. 2D). Latrunculin sequesters actin monomers, preventing reassembly, and thus more readily causes loss of actin structures with higher filament turnover (fast dynamics; see Materials and Methods for optimization of the conditions). In untreated cells, the junctional actin and thin bundles were clearly seen (DMSO, see enlargement, Fig. 2D). After treatment with latrunculin for 5 minutes, junctional actin had mostly disappeared from sites of adhesion, whereas thin bundles are still present (but qualitatively different from controls). After 15 minutes of new contact formation in the presence of latrunculin, there was a fourfold reduction in the proportion of cells that contained junctional actin (Latr. enlargement, Fig. 2D,E). However, remnants of thin bundles were still observed in around 60% of keratinocytes (arrows, Latr., Fig. 2D,E). Thus complete disassembly of thin bundles (>15 minutes) takes much longer than disassembly of junctional actin (5 minutes). This result is consistent with the analysis of labelled actin incorporation (Fig. 2A-C) and suggests that flanking bundles are more stable and have slower turnover than junctional actin.

In assessing the effect on junctional actin, it is important to distinguish whether latrunculin prevents actin recruitment to puncta or the process of receptor clustering itself. To distinguish between these possibilities, as control we clustered cadherin receptors using antibody-coated beads, a process known to recruit actin and mimic early signalling events after contact assembly (supplementary material Fig. S3) (Betson et al., 2002; Braga et al., 1997). In the presence of latrunculin, actin recruitment is unable to occur, even though cadherin receptors are clustered around the beads (supplementary material Fig. S3). Thus, latrunculin treatment affected primarily new actin polymerization at puncta and not cadherin clustering per se. These results indicate that cadherin clustering is indirectly perturbed when actin recruitment is inhibited by latrunculin, leading to the removal of cadherin receptors from cell-cell contacts (as seen in Fig. 2D). The concentration of calcium ions in the medium did not affect actin recruitment substantially, in spite of the reported increase in intracellular calcium levels (supplementary material Fig. S3) (Sharpe et al., 1993). Taken together, the above results indicate that, following cadherin-dependent adhesion, actin polymerization occurs at two distinct intracellular sites with different dynamics: at cell-cell contacts (faster dynamics) and at flanking bundles (slower dynamics).

What is the contribution of assembly mechanisms to junctional actin and thin bundles?

Actin assembly mechanisms were addressed in terms of the G- to F-actin ratio, filament polarity of actin polymerization and supply of actin monomers to fuel polymerization (Figs 3, 4). Under our conditions, G- and F-actin can be extracted, and, as expected, latrunculin treatment (as per Fig. 2D) results in a twofold increase in the levels of G-actin (Fig. 3A) (Cramer et al., 2002). Thus, our conditions are adequate to detect changes in the G- to F-actin ratio.

Initially, we investigated whether junction formation increased the total levels of polymerized actin in keratinocytes (F-actin) during a time course of junction assembly (Fig. 3B,C). Apart from a slight alteration at 15 minutes, the ratio

of monomeric and filamentous actin did not vary after induction of cell-cell adhesion (G-actin and F-actin, respectively; Fig. 3C). These results suggested that there is not a major shift towards actin polymerization or depolymerization during junction formation. However, it is clear that junction formation induces new actin polymerization at puncta (Fig. 2) (Adams et al., 1996; Braga et al., 1997). Most probably this localized process is beyond the sensitivity of the global methods used in this study and reflects the small proportion of total actin at junctions. Indeed, when G- and F-actin pools were

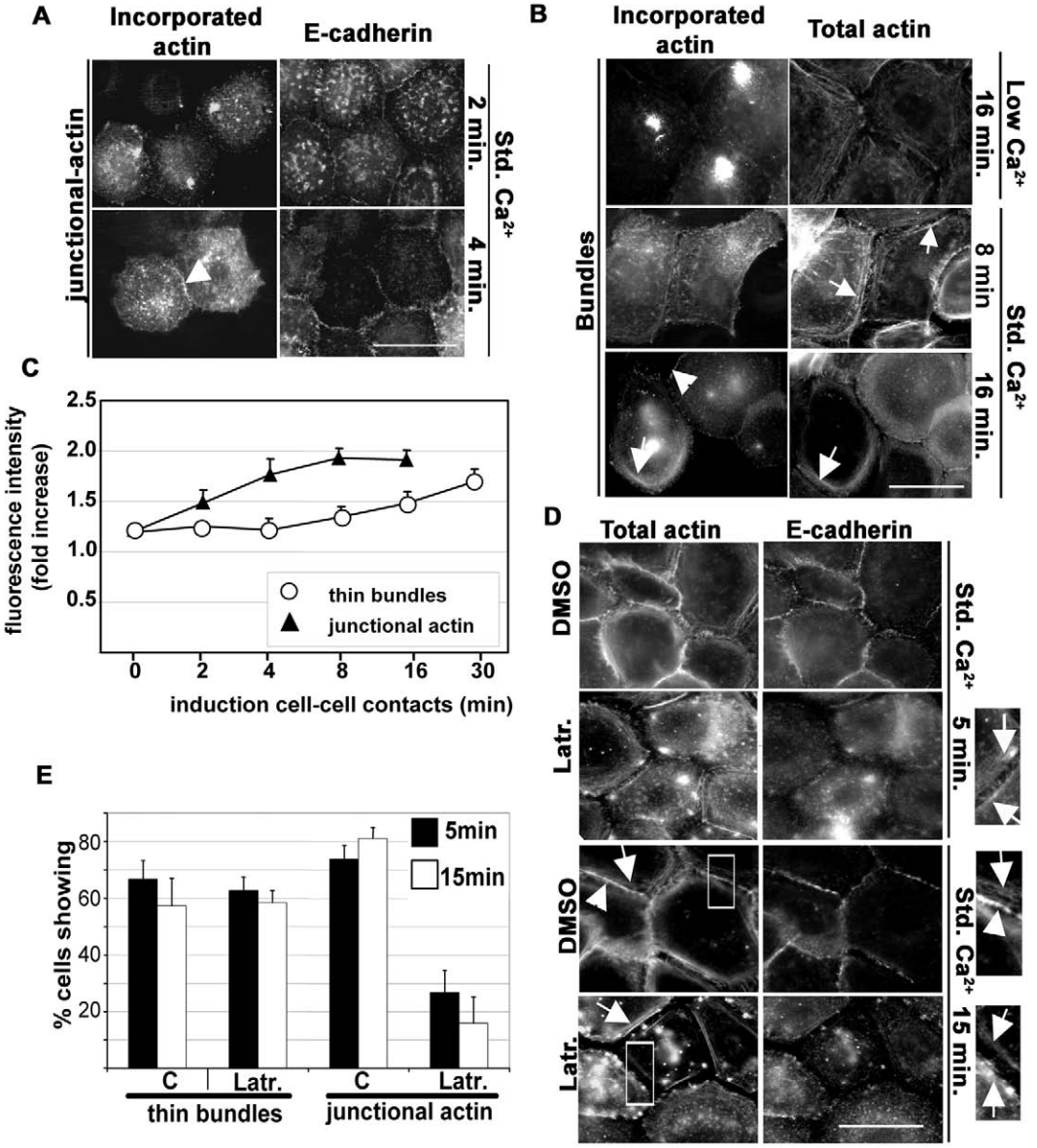

Fig. 2. Junctional actin and thin bundles have distinct dynamics. Keratinocytes grown in low calcium medium (Low Ca^{2+}), which does not induce cell-cell contacts were microinjected with labelled actin (3 mg/ml pipette concentration), and transferred immediately to standard calcium medium to induce cell-cell contacts (Std. Ca^{2+}). Control cells were maintained in low calcium medium. Arrowheads point to junctional actin; arrows show thin bundles. (A) Junctional actin has fast dynamics. After junction formation, images were collected at places where E-cadherin clustering was visible and at the corresponding incorporated actin. (B) Thin bundles have slower kinetics of actin incorporation. Images were collected where filamentous actin (total actin) was present and the corresponding new actin labelling at the bundles (incorporated actin). In the absence of cell-cell contacts (Low Ca^{2+}), very little actin incorporation was detected into thin bundles. (C) Quantification of actin dynamics. Junctional-actin fluorescence intensity was measured only where cadherin recruitment at junctions was observed. Thin bundles were detected in phalloidin stained images and the fluorescence intensity of labelled actin was measured in the corresponding area. (D) Thin bundles are less sensitive than junctional actin to latrunculin treatment. Keratinocytes were induced to form contacts (5 and 15 minutes, Std. Ca^{2+}) in the presence of 0.2 μM latrunculin B (Latr.) or vehicle (DMSO); cells were fixed and stained with phalloidin (total actin) and anti-E-cadherin antibodies. Although the amount and organization of thin bundles are affected by latrunculin, thin bundles are clearly seen after 5 minutes incubation, when the majority of junctional actin was removed. (E) Quantification of the proportion of cells showing thin bundles and junctional actin in controls (C) or after latrunculin treatment (Latr., at 5 and 15 minutes). Error bars represent error obtained from at least two independent experiments. Bar, 50 μm.

quantified specifically at cell-cell contacts, a significant increase in the F-actin pool was observed when compared to F-actin levels in the absence of cell-cell adhesion (time 0 minutes, $P<0.05$, Fig. 3C).

We next investigated the contribution of the two spatial actin populations detected to filament assembly at filament barbed and pointed ends, as both filament ends have been shown to be competent for assembly in other cell systems (Littlefield et al., 2001). We tested this by briefly permeabilizing keratinocytes with a buffer containing labelled actin in the presence or absence of cytochalasin B (Fig. 3D) (Chan et al., 2000). To assess the assembly at filament-barbed ends (the expected preferred site of assembly) we used labelled actin at 0.45 μM, which is well below the critical concentration for assembly at the pointed end (around 1 μM) and thus only allows assembly at the barbed end. Cytochalasin B binds to the barbed ends and prevents polymerization at these sites, but allows incorporation at filament pointed ends (Littlefield et al., 2001). Importantly, the brief treatment with cytochalasin B (2 minutes) is sufficient to block barbed ends but does not disrupt actin structures inside the cell (total actin, Fig. 3D).

In the absence of cell-cell contacts (Low Ca^{2+}), no incorporation of actin was observed (Fig. 3D). When junctions were induced in the absence of cytochalasin B, junctional actin was labelled as early as 5 minutes and the intensity of labelling and proportion of labelled cells increased with time (up to 60 minutes, arrows Fig. 3D and data not shown). At all time points, punctate labelling was heterogeneous, colocalized with newly formed cadherin-dependent cell-cell contacts, and thus reflects incorporation into junctional actin (Fig. 3D). Treatment with cytochalasin B substantially reduced actin labelling at cell-cell adhesion sites (incorporated actin). The residual actin labelling can be accounted for by a small proportion of G-actin we found at junctions (data not shown). Actin incorporation

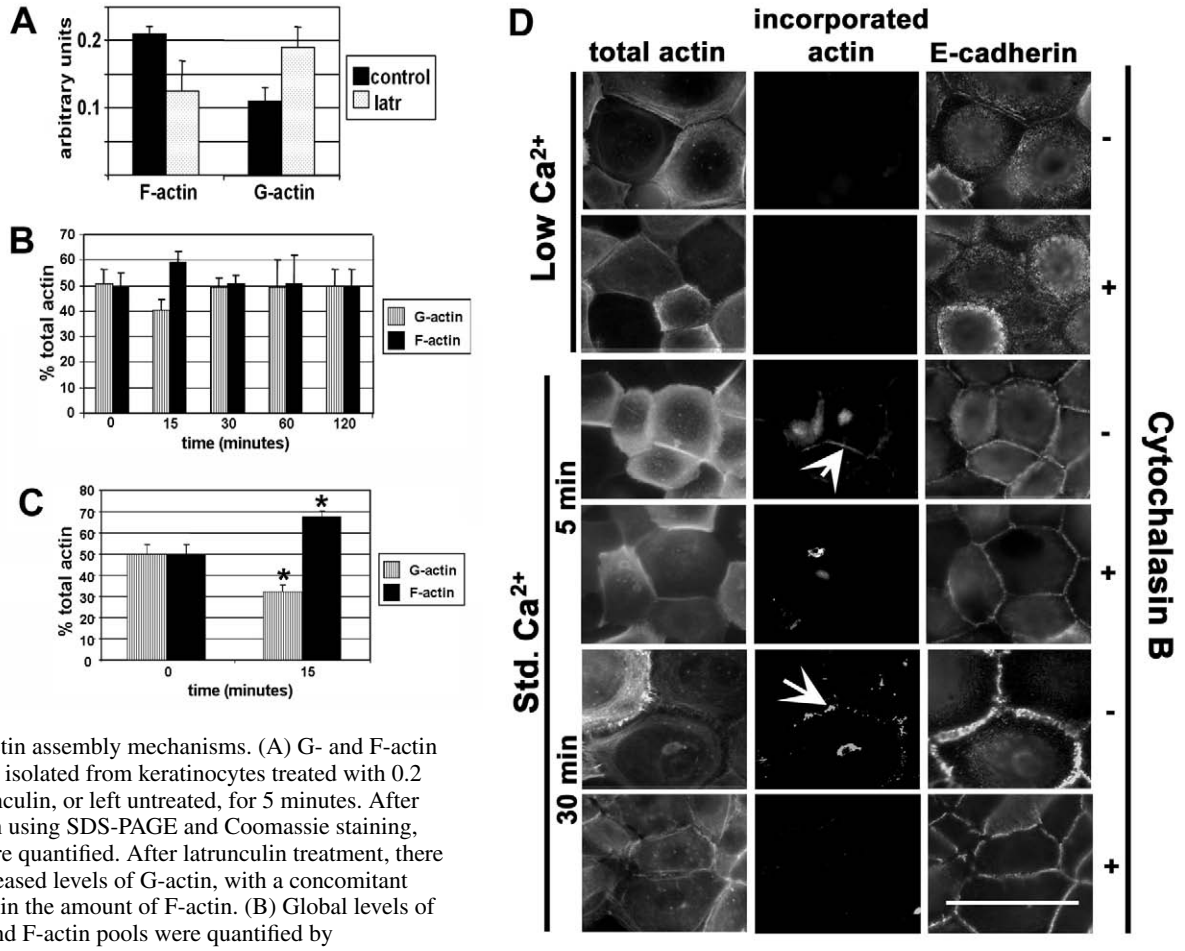

Fig. 3. Actin assembly mechanisms. (A) G- and F-actin pool were isolated from keratinocytes treated with 0.2 μM latrunculin, or left untreated, for 5 minutes. After separation using SDS-PAGE and Coomassie staining, bands were quantified. After latrunculin treatment, there were increased levels of G-actin, with a concomitant reduction in the amount of F-actin. (B) Global levels of G-actin and F-actin pools were quantified by immunofluorescence during a time course after induction of cell-cell contacts. Keratinocytes were stained with DNAse1 (G-actin) and phalloidin (F-actin) and the whole optical field quantified for each fluorophore. No significant changes were observed in the relative concentration of either actin pool during the time course examined by staining or SDS-PAGE (data not shown). Values are expressed as percentage of total actin. (C) Quantification of immunofluorescence of G- and F-actin pools at the junctional-actin region. Only junctions where junctional actin was clearly separated from thin bundles were examined. At time zero, areas of close apposition of neighbouring membranes were quantified. Data in A-C are representative of two independent experiments. Error bars represent standard deviation. *$P<0.05$. (D) Polymerization of actin at cell-cell junctions occurs preferentially via the barbed end. After formation of new contacts for different amounts of time, cells were permeabilized for 2 minutes in cytoskeleton buffer containing labelled Alexa Fluor 568-G-actin (0.45 μM), in the presence or absence of 2 μM cytochalasin B (see text for details). After fixation, E-cadherin, total actin (phalloidin) and incorporated actin were visualized. Results are representative of at least three independent experiments. Arrows indicate labelled actin incorporation at junctions. Bar, 50 μm.

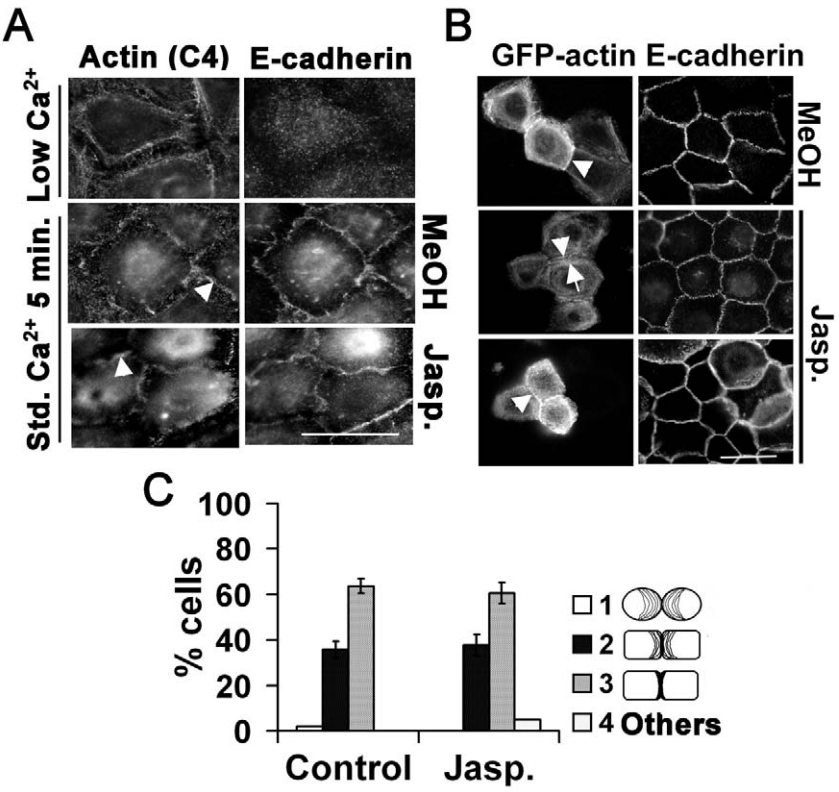

Fig. 4. Actin filament disassembly does not play a major role in the formation of either thin bundles or junctional actin. (A) Recently disassembled filaments do not contribute monomers for incorporation at cell-cell junctions. Cell-cell contacts were induced (Std. Ca^{2+}) in the presence of 0.5 μM jasplakinolide (Jasp.) or vehicle control (methanol, MeOH). Cells were stained with anti-E-cadherin and anti-actin antibodies, because jasplakinolide competes with phalloidin for F-actin interaction. (B) Actin disassembly is not required for bundle reorganization. Keratinocytes expressing GFP-actin were treated with 0.02 μM jasplakinolide (Jasp.) or methanol (MeOH) during junction assembly. After 60 minutes, thin bundles were visible either as flanking filaments to junctional actin (middle images Jasp.) or coincident to junctions (bottom images, Jasp.). Arrows indicate thin bundles; arrowheads point to junctional actin. (C) Keratinocytes were classified into four different categories according to the spatial localization of thin bundles as described in Fig. 1 legend. The same proportion of cells was found in category 2 and 3 for both the Jasplakinolide-treated (Jasp.) and untreated (control) cells. Bar, 50 μm.

appeared to reach a steady state after 1 hour of cell-cell adhesion formation (data not shown). As expected from the short pulse of labelling (2 minutes) and the known half-life (Fig. 2C), no bundles were labelled under these conditions. Taken together, these results indicated that junctional actin is assembled by new actin polymerization at barbed ends.

Actin filament disassembly does not play a major role in the formation of either thin bundles or junctional actin

During junction assembly, actin monomers from two distinct sources can potentially contribute to the newly polymerized actin: previously stored monomers, newly disassembled actin, or both. To determine whether recently disassembled actin filaments might contribute monomers for recycling and reassembly at junctions, actin filaments were stabilized by treatment with jasplakinolide (see Materials and Methods for titration; Fig. 4). After induction of contacts in the presence of jasplakinolide for up to 15 minutes (a time when both actin populations are detectable), junctional actin was observed in a similar pattern to that found for controls (arrowhead, Std. Ca^{2+}, Fig. 4A and data not shown).

To overcome the poor labelling of bundles by anti-actin antibody (C4), GFP-actin was expressed in keratinocytes and cells incubated with jasplakinolide during induction of cell-cell contacts for 60 minutes (Fig. 4B). At this time, the two spatially distinct populations of actin will be detectable in a proportion of cells whereas in others the two actin populations will be coincident (Fig. 1). When jasplakinolide-treated keratinocytes were compared with controls, there was not much difference in the percentage of cells in which bundles and junctional actin were no longer distinguishable (category 3, Fig. 4C). Thus, our data indicate that bundles are not disassembled and reassembled at a position closer to junctional actin during maturation of contacts. Moreover, our results suggested that actin depolymerization is not a major supply of actin monomers for incorporation in either junctional actin or thin bundles.

What is the contribution of myosin contractility to junctional actin and bundles?

When myosin II was inhibited (by blocking myosin light chain kinase), no effect on the clustering of cadherin receptors at puncta (Vaezi et al., 2002) or maintenance of stable, already assembled junctions was found (Bhowmick et al., 2001; Krendel et al., 1999; Sahai and Marshall, 2002). Here, we addressed the role of contractility for the formation of the two actin populations. We selected blebbistatin, a newly characterized inhibitor of myosin II (see Materials and Methods for optimization) (Straight et al., 2003), which is advantageous over previous myosin II inhibitors as it directly blocks myosin II ATPase, is rapid, and highly specific (Straight et al., 2003).

Bundles are clearly detected in controls (DMSO, insets, Fig. 5), but not in blebbistatin-treated keratinocytes (*, insets, Fig. 5). In contrast, junctional actin was able to form at sites of cell-cell contact (arrows, Bleb., inset, Fig. 5). However, junctions that formed in the presence of blebbistatin appeared less robust, with weaker and more punctate actin/cadherin staining instead of a continuous line as seen in controls (arrowheads, Bleb., Fig. 5). We also obtained similar results when using other myosin II inhibitors (Y27632 and ML9; data not shown). However, the blebbistatin effects were more potent and observed

homogeneously throughout the monolayer. Thus, myosin II contractility is not required for junctional-actin assembly, but is essential for thin bundle stability.

We stained with phosphorylated myosin light chain (P-MLC) to test which of the actin population was contractile during induction of cell-cell contacts. In cells without adhesion there was minimal localization of P-MLC in peripheral bundles (Low Ca^{2+}, Fig. 6), indicating that bundles formed prior to contact initiation are not contractile. In contrast, once contacts were initiated, P-MLC was abundant on peripheral actin bundles (arrows, 30 and 60 minutes, Fig. 6). Interestingly, P-MLC was clearly absent from junctional actin (asterisks, Fig. 6). These results are also consistent with the ability of cadherin receptors to recruit and assemble actin at cell-cell contacts in the absence of myosin function (Fig. 5).

We next quantified the increase in P-MLC levels after induction of cell-cell contacts, using western blots and confocal images. After 30 minutes of junction formation, the intensity of P-MLC fluorescence at thin bundles was 2.7-fold higher than levels seen at bundles in the absence of cell-cell adhesion (Low Ca^{2+}, Fig. 7A). A smaller increase in P-MLC levels was also observed in the cell body (1.4 fold, Fig. 7A). Furthermore, overall levels of P-MLC were also increased, as seen by western blots (Fig. 7B). Thus enhanced P-MLC levels can be detected both spatially and globally after junction assembly, but the increase in phosphorylated MLC is most marked at thin bundles.

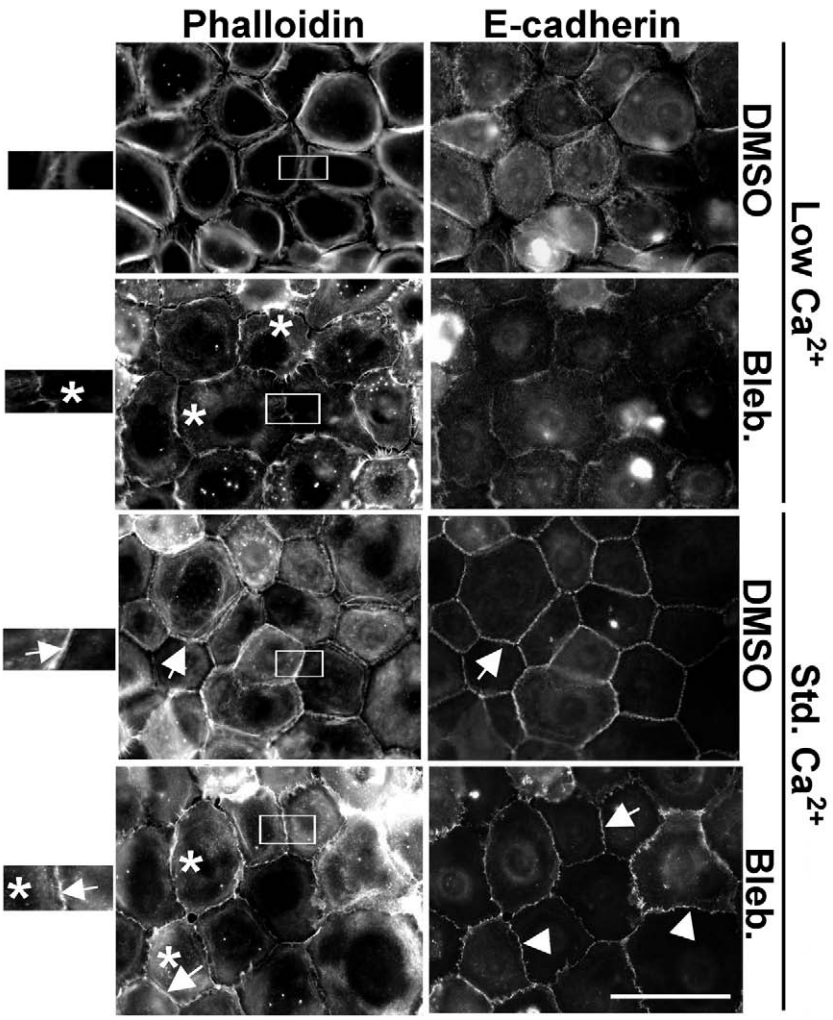

Fig. 5. Contribution of myosin contractility to junctional actin and thin bundles. Confluent keratinocytes grown in low calcium medium (Low Ca^{2+}) or induced to form junctions (Std. Ca^{2+}) for 1 hour were incubated in the presence or absence of blebbistatin (Bleb.). Controls were treated with DMSO. Enlargements of the boxed regions in each image are shown on the right. In the absence of cell-cell contacts (Low Ca^{2+}) thin bundles are present in control (DMSO-treated) cells, but not in blebbistatin-treated cells (Bleb.) After cell-cell adhesion, junctional actin is formed in the absence of thin bundles (Bleb. Std. Ca^{2+}). Asterisks indicate the absence of thin bundles in blebbistatin-treated keratinocytes; arrow indicates junctional actin and arrowheads, wavy junctions. Images are representative of at least three independent experiments. Bar, 50 μm.

What is the role of actin bundles during epithelial polarization?

The recognition of actin bundles flanking junctional actin and their progressive bundling during junction formation is newly described and thus we began to investigate their function. As thin bundles are not required for the initial actin recruitment to junctions (Fig. 5), a function during the later stages of epithelial polarization was investigated. We focused on the formation of the cuboidal morphology, the major cell shape change that occurs during the maturation step of polarization.

A cuboidal morphology is achieved when cell-cell contacts form a distinct, tall lateral domain perpendicular to the base of the cell. We sought to evaluate whether inhibition of contractility during junction assembly could affect the height of lateral domains during polarization. Confocal Z-series of keratinocytes incubated in the presence or absence of blebbistatin during induction of cell-cell contacts were collected and used for 3D reconstructions or quantification (Fig. 8). Control cells show a uniform linear staining for E-cadherin coincident with junctional actin (control, Fig. 8A). Blebbistatin treatment induced the breakdown of thin bundles and the formation of small ruffles all over the cell surface, but particularly concentrated at sites of cell-cell contacts (blebbistatin, arrows, Fig. 8A,B). Underneath the small ruffles, cadherin-dependent contacts were present as a continuous thinner line (Fig. 8B),

Z-projections are usually used to determine cell height. However, the presence of small ruffles on top of junctions prevented quantification of cell height in this manner. To circumvent this problem, we measured the height of the lateral domain, which increases upwards during polarization to form a cuboidal morphology. We quantified the number of confocal sections (0.3 μm) in which linear, continuous cadherin staining is seen (basal to apical distance, Fig. 8B,C). Cells maintained in low calcium medium show a small area of contact between

neighbours, presumably mediated by calcium-independent receptors (around 2 μm high) (Braga et al., 1998). Following induction of cell-cell contacts for 1 hour, control keratinocytes were not yet fully cuboidal (lateral domain was around 4.5 μm high as opposed to 6 μm measured at the apex on top of the nucleus of the cell). After inhibition of myosin II-dependent contractility, the height of the lateral domain was reduced by around 35% to 3 μm (P<0.001, Fig. 8C). Thus, an increase in height of the lateral domain during polarization requires the presence of acto-myosin bundles.

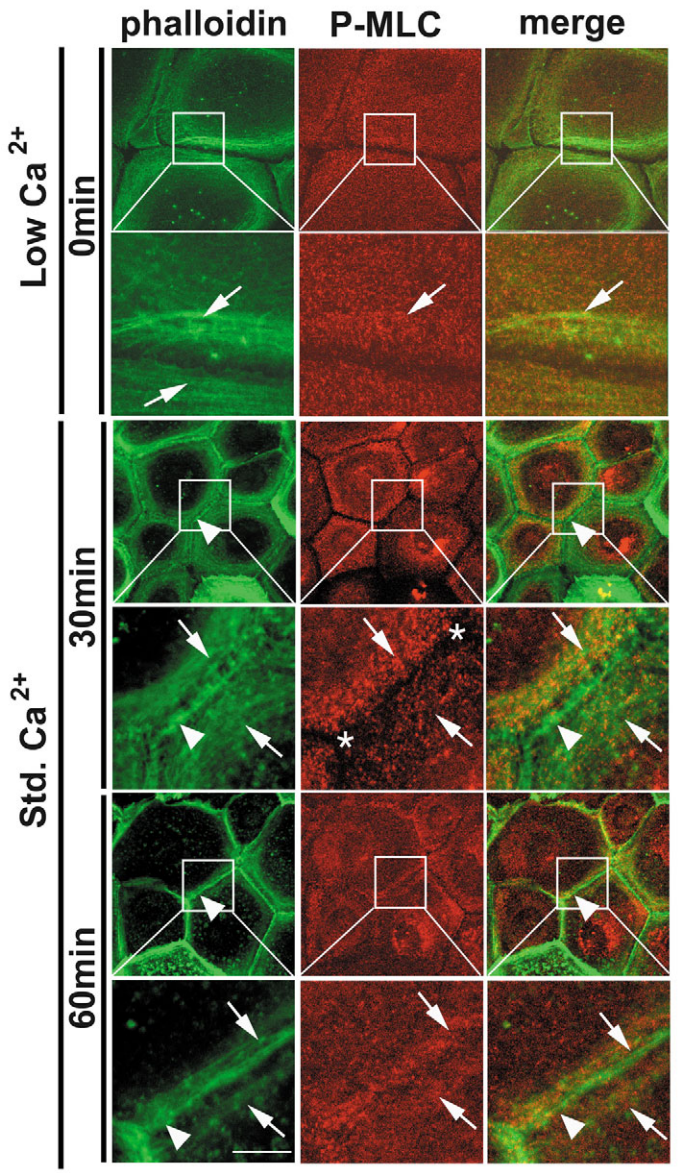

Fig. 6. Following cell-cell junction formation, phosphorylated myosin light chain (P-MLC) localizes at thin bundles but not junctional actin. Keratinocytes grown in low calcium medium (Low Ca^{2+}) were induced to form junctions (Std. Ca^{2+}) and stained with phalloidin and anti-P-MLC. Merged confocal images are shown on the right; Enlargements of the boxed regions are shown below each image. After induction of cell-cell contacts, P-MLC is concentrated at peripheral thin bundles, but absent from junctional actin (Std. Ca^{2+}). Arrowheads show junctional actin, arrows point to thin bundles and localization of P-MLC. Asterisks show absence of P-MLC at junctional actin. Bar, 32 μm; 8 μm for enlargements.

Discussion

We demonstrate that, after initial cell-cell contact in confluent keratinocytes, epithelial morphological polarization is induced rapidly. During keratinocyte polarization, we found two spatial actin populations, junctional actin and thin bundles, which can be distinguished by their dynamics, molecular components, mechanism of formation and function (Fig. 1, Fig. 9A and supplementary material Fig. S2). We define junctional actin as a higher order of puncta organization forming a linear array of actin staining at junctions. Although E-cadherin clustering is the initial trigger for punctum assembly, additional receptors present at cell-cell contacts also contribute to actin recruitment to form junctional actin. Thin bundles are a pre-formed array of loosely associated actin filaments found in the absence of cell-cell contacts, distinct from stress fibres in their spatial organization.

Within 1 hour, discrete, stepwise and sequential changes in the actin cytoskeleton occur (Fig. 9). Similar actin populations and microfilament reorganization are observed in sub-confluent cultures, but a lag phase is seen as cells have to

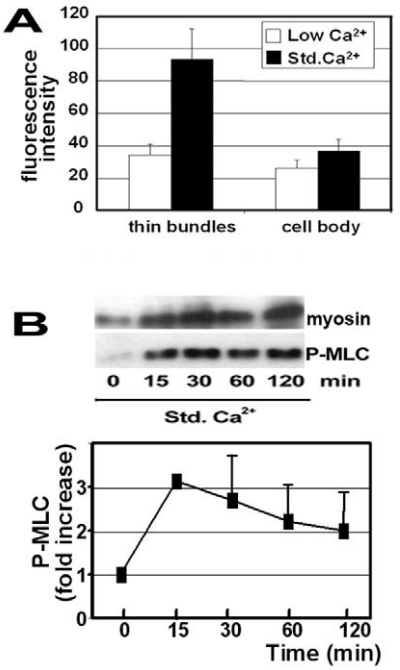

Fig. 7. Spatial and global quantification of P-MLC levels during keratinocyte polarization. (A) P-MLC levels were quantified at thin bundles and in the cell body from confocal images obtained after 30 minutes of induction of cell-cell contacts. Following junction formation (Std. Ca^{2+}), an increase in fluorescence intensity is seen both at thin bundles (2.7 fold) and in the cell body (1.4 fold). Values are from two independent experiments, using at least 50 different cells per condition. (B) Western blots showing the overall increase in P-MLC levels in keratinocytes. Quantification reveals that a threefold increase in phosphorylation levels is seen after 15 minutes of new junction formation (P<0.001). Values are the mean of four independent experiments.

migrate towards each other prior to initiation of junctions (Fig. 1C). Thus the results described here are likely to be important for junction formation in general, i.e. following cytokinesis, resealing of epithelial sheets, wound healing and mesenchymal-epithelial conversion during development.

Junctional actin has fast dynamics while thin bundles show slow incorporation of monomers. Actin incorporation at cell-cell junctions ($t_{1/2}$=3 minutes) is slightly longer than incorporation of labelled actin in lamellipodia (Adams et al., 1998; Adams et al., 1996; McNeill et al., 1993; Theriot and Mitchison, 1991). The slow kinetics of incorporation into thin bundles ($t_{1/2}$=12 minutes) is similar to that observed into stress fibres (Amato and Taylor, 1986) and circumferential rings in a cultured epithelial cell line (L.P.C., unpublished data).

To what extent the actin structures we observe are further related to other actin structures remains to be directly tested. Flanking actin bundles are more related to circular actin rings than stress fibres because of their peripheral spatial distribution and circular orientation within cells. A common theme for actin incorporation at new cell-cell contacts, lamellipodia and filopodia is that assembly occurs with filament barbed ends facing the plasma membrane. However, further filament elongation differs in that junctional actin filament elongation is apparently restricted to within sub-microns of the cell edge, whereas lamellipodia and filopodia can be 2-10 μm deep. This infers differences in precise regulation of actin incorporation, spatial orientation of filament growth and/or length of filaments.

With respect to the mechanism of formation of junctional actin and thin bundles (Fig. 9A), our findings on actin incorporation and latrunculin argue that actin filament assembly is a major contributor to junctional actin, but less important for flanking bundles (the latter has reduced sensitivity to latrunculin and thus less reliance on rapid assembly for formation). Actin filament disassembly has no clear role for the formation of either actin population, suggesting that the required monomer for incorporation is supplied from the stored pool of actin monomer (as opposed to recently disassembled actin filaments). Conversely, myosin II function is apparently more important for bundle formation: thin bundles dissolve when myosin II is inhibited, but actin recruitment at new junctions can occur (this work) (Vaezi et al., 2002). In addition, myosin II-induced contraction is not relevant to the initial clustering of cadherins at sites of cell-cell contacts.

How exactly does myosin II contribute to flanking bundle reorganization? Given that actin assembly plays only a minor role and disassembly of filaments is not required, a mechanism that relies at least in part on pre-existing filaments seems likely. One idea is a progressive bundling of pre-existing filaments (loose array of filaments observed in cells prior to junction formation, Fig. 9B). While we can not exclude the participation of bundling proteins in this process, myosin II-induced contractility does play a role. Support for this comes from increased levels of P-MLC at bundles (2.7-fold, Fig. 7A) and a progressive narrowing of the loose band of filaments towards

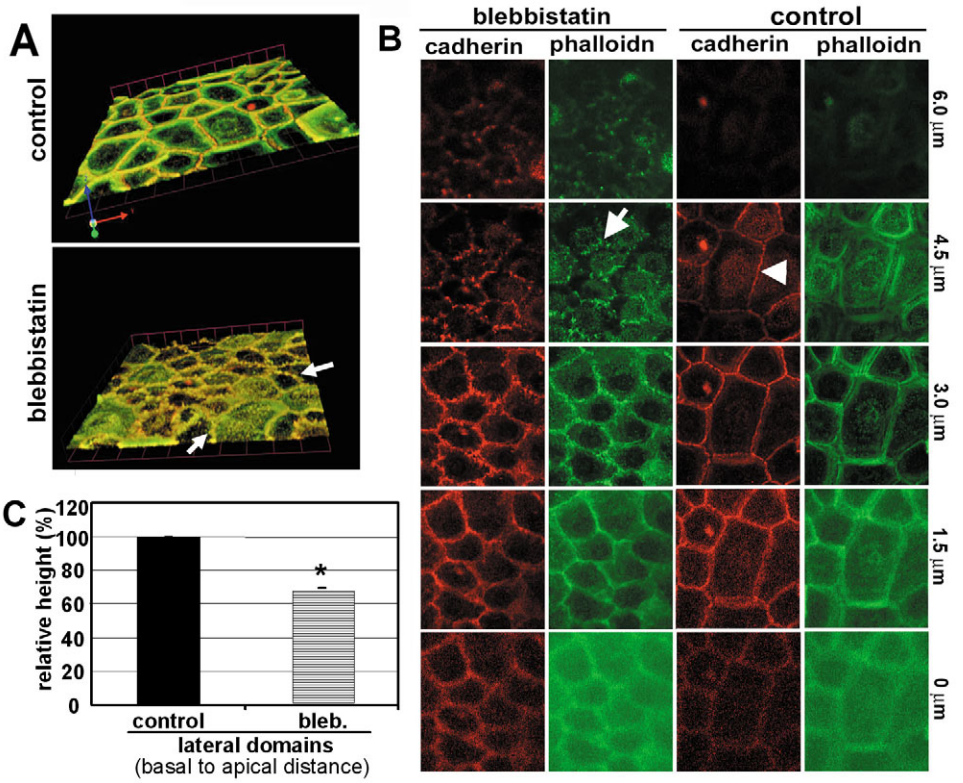

Fig. 8. Inhibition of contractility during keratinocyte polarization perturbs the acquisition of maximum height at lateral domains. E-cadherin (red) and phalloidin (green) staining was performed after 1 hour of cell-cell contact formation in the absence (control) or presence of blebbistatin (blebbistatin). Confocal sections (0.3 μm) were collected at different levels through a keratinocyte monolayer and processed as follows. (A) Three dimensional reconstruction. After blebbistatin treatment, F-actin is diffusely localized and cadherin staining is found as a wavy line between neighbouring cells. Small ruffles/projections are seen at the cell surface and on top of junctions (arrows). (B) Confocal sections taken from basal to top of the monolayer at 0, 1.5, 3, 4.5 and 6 μm. Arrow points to small ruffles/projections sees at the top of junctions. Arrowhead shows cadherin staining in controls whereas no similar linear cadherin staining is observed in blebbistatin-treated cells. (C) Quantification of the maximum height of the lateral domains (basal to apical distance). Confocal sections showing linear cadherin staining were quantified and values expressed relative to control, untreated cells polarized for 1 hour (see Materials and Methods for details). Maximum height seen in lateral domain of control cells is 4.5 μm compared with 3 μm in blebbistatin-treated cells and 2 μm in cells maintained in low calcium (Braga et al., 1998). After blebbistatin treatment, lateral domain height is decreased by 35% (*P<0.001). Results represent the mean of seven different Z-series collected from two independent experiments.

junctional actin shortly after junctions are assembled (Fig. 1, Fig. 9B). Significantly, peripheral actin bundles are only contractile once contacts are initiated (Fig. 6, Fig. 7A), inferring signalling to myosin II to activate contraction at bundles

The above mechanism differs from models in the literature in which disassembly/reassembly of bundles at a location closer to junctions is proposed (Krendel et al., 1999; Krendel and Bonder, 1999). This discrepancy may be explained by the fact that in these studies, cells migrate to adhere to their neighbours. Thus different/additional pathways for actin formation may occur in sub-confluent cultures until junctional actin is stabilized, whereas we can exclude motility in our experimental system (see Fig. 1).

One important issue is that we do not yet know whether junctional actin and thin bundles co-exist as separate dynamic populations beyond the formation of a mature junction by 1 hour. We favour the co-existence of the two populations as actin bundles and mature junctions themselves can be resolved by electron microscopy (Green et al., 1987; Owaribe et al.,

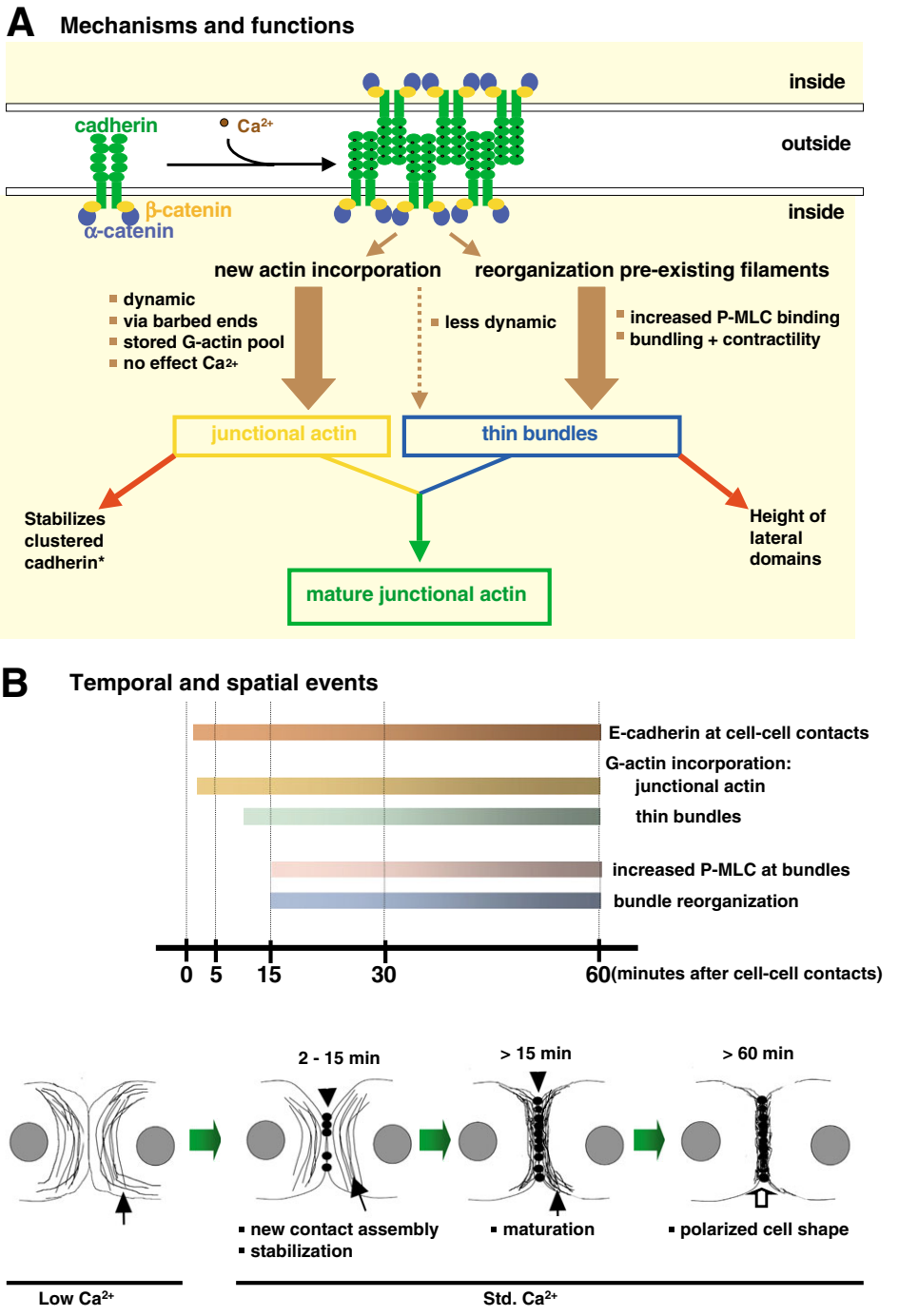

Fig. 9. Summary of changes to the microfilament network triggered by formation of cadherin-dependent cell-cell contact. (A) Mechanisms of formation and functions of junctional actin and thin bundles. After cadherin receptors cluster, two distinct processes are observed: new actin polymerization and filament reorganization. Actin assembly is a major contributor to junctional actin (thick brown arrow), but has a minor effect on thin bundles (dashed thin brown arrow). In contrast, myosin function is essential for bundle stability, but does not affect initial clustering of cadherin receptors or junctional-actin formation. All the above events do not occur in cells maintained in low calcium medium or in which cadherin function is blocked. Two separate functions are identified (red arrows): junctional actin stabilizes cadherin receptors at puncta and thin bundles are essential for development of maximum height of the lateral domains. At later time points, these two actin populations apparently colocalize at cell-cell contacts to form mature junctional actin (merged blue and yellow lines; see below). *Adams et al., 1996; Nelson, 2003. (B) Temporal and spatial events. After initiation of cell-cell adhesion, distinct cellular processes are detected at different time points (horizontal bars). Once initiated, each event increases until a plateau after 60 minutes of cell-cell adhesion. E-cadherin clustering at puncta is observed within a couple of minutes, and is followed shortly by new actin incorporation as junctional actin ($t_{1/2}$=3 minutes, fast dynamics) and then by thin bundle labelling (approximately $t_{1/2}$=12 minutes; slower dynamics). Increased P-MLC localization at bundles and bundle reorganization occurs later (from 15 minutes). The end result is the formation of a cuboidal epithelial morphology, with the spatial organization of microfilaments as shown. A possible mechanism, supported by our results, is myosin-dependent contraction of thin bundles from a loose band of filaments at the periphery to filaments that are coincident with junctional actin. Please see text for functional implications and more details. Arrows indicate bundles; arrowheads indicate junctional actin, open arrow indicates mature junctional actin.

1981; Yonemura et al., 1995; Zamansky et al., 1991). Thus in mature junctions, the thick bundles visualized by immunofluorescence result from the contribution of junctional actin and compacted, bundled thin filaments.

Presumably, as myosin contraction is required for bundling and bundles later coincide with junctional actin, myosin II may have some indirect role in junctional-actin stability (but not assembly per se). This is perhaps observed as a more irregular distribution of junctional actin (this work), and junction morphology has an immature, wavy shape when myosin II is blocked (Fig. 5) (Krendel et al., 1999; Vaezi et al., 2002; Yonemura et al., 1995). Further experiments are needed to validate whether the coalescence of distinct puncta into a straight, continuous line requires acto-myosin-generated tension.

While the function of actin at puncta has been previously identified, so far no specific role for bundles has been assigned. Here, we suggest a novel role for thin bundle reorganization and actomyosin contraction in the development of epithelial morphology: increase in height of the lateral domain to form a cuboidal cell. We argue that this is a specific function of flanking bundles. First, blebbistatin treatment maintains the lateral domain at similar height to cells grown in low calcium medium (around 2-3 μm) as opposed to control cells polarized for 1 hour (Fig. 8) (Braga et al., 1998). Second, following junction assembly, thin bundles are the major contractile actin population detected, as opposed to junctional actin (Figs 6, 7). Third, the apparent progressive bundling of filaments and increase in MLC phosphorylation are temporally coincident (Fig. 9B). This argues strongly that bundling and contraction of actin bundles correlate with the increase in height of the lateral domain and cuboidal morphology. However, additional roles for thin bundles may yet be uncovered, such as the potential crosstalk with junctional actin mentioned above.

Thus, the cytoskeletal changes reported here occur quickly (within 1 hour), in a precise sequence that reflects their requirements and specific functions (Fig. 9B). We concluded that during epithelial polarization, the formation of actin structures at junctions is achieved by cooperation of contraction and assembly of two spatially distinct actin populations (Fig. 9A). Similar cooperation between actin assembly and myosin II contractility for overall cell function occurs in other cell systems, such as cell migration (Ridley et al., 2003) and healing of circular wounds in *Xenopus* oocytes (Mandato and Bement, 2001).

The proposed contractile role of the newly described thin bundles in polarization is consistent with the importance of cell contraction for epithelial morphogenesis: compaction (Adams et al., 1998; Clayton et al., 1999; Collins and Fleming, 1995), tubulogenesis (Wozniak et al., 2003) and elongation in *C. elegans* (Wissmann et al., 1999). In addition, during junction assembly in primary keratinocytes up-regulation of Rho small GTPase activity occurs (data not shown) (Calautti et al., 2002). Interestingly, in tumorigenic and non-tumorigenic cell lines Rho is not activated after cadherin adhesion (Noren et al., 2001), and instead increased contractility may disrupt cell-cell contacts (Sahai and Marshall, 2002; Zhong et al., 1997). Yet, in some cell lines it has been proposed that increased contractility may disrupt cell-cell contacts (Sahai and Marshall, 2002; Zhong et al., 1997). These results suggest that a tight temporal and spatial regulation of Rho activation and contractility is required for epithelial homeostasis and morphogenesis.

Our data show that cadherin-mediated adhesion is able to modulate actin dynamics. After cell-cell contacts are initiated, an increase in actin turnover, new actin incorporation, myosin II phosphorylation, contraction and bundling are observed (Fig. 9A). These events are focused on two different actin populations, junctional actin and thin bundles that, at early time points during keratinocyte polarization, can be separated mechanistically (Fig. 9A) and spatially (Fig. 9B). Most importantly, the unique roles of junctional actin (cadherin clusters stability) and thin bundles (height increase at lateral domains) cooperate to induce overall morphological change (cuboidal cell shape). Thus, following keratinocyte junction assembly, two actin populations with two distinct functions are required to develop a polarized epithelial cell.

We would like to thank T. Mitchison, M. Takeichi, L. Machesky, M. Matsuda and A. Yoshimura for generous gift of reagents. We thank Y. Korchev and J. Gorelik for discussions and suggestion of cell height experiments. V.B. is a MRC Senior Research Fellow; M.B. was a PhD student from the graduate programme at the MRC Laboratory for Molecular Cell Biology, University College London. L.C. is a Royal Society University Research Fellow. This work was generously supported by the Medical Research Council to V.B. and by the Wellcome Trust, Human Frontiers Science Programme Organization and the Royal Society (UK) to L.C.

References

Adams, C. L., Nelson, W. J. and Smith, S. J. (1996). Quantitative analysis of cadherin-catenin-actin reorganization during development of cell-cell adhesion. *J. Cell Biol.* **135**, 1899-1911.

Adams, C. L., Chen, Y.-T., Smith, S. J. and Nelson, W. J. (1998). Mechanisms of epithelial cell-cell adhesion and cell compaction revealed by high-resolution tracking of E-cadherin-green fluorescent protein. *J. Cell Biol.* **142**, 1105-1119.

Amato, P. A. and Taylor, D. L. (1986). Probing the mechanism of incorporation of fluorescently labeled actin into stress fibers. *J. Cell Biol.* **102**, 1074-1084.

Betson, M., Lozano, E., Zhang, J. and Braga, V. M. M. (2002). Rac activation upon cell-cell contact formation is dependent on signaling from the epidermal growth factor receptor. *J. Biol. Chem.* **277**, 36962-36969.

Bhowmick, N. A., Ghiassi, M., Bakin, A., Aakre, M., Lundquist, C. A., Engel, M. E., Arteaga, C. L. and Moses, H. L. (2001). Transforming growth factor-β1 mediates epithelial to mesenchymal transdifferentiation through a RhoA dependent mechanism. *Mol. Biol. Cell* **12**, 27-36.

Braga, V. (2000). Cadherin adhesion regulation in keratinocytes. In *Cell-Cell Interactions: a practical approach* (ed. T. Fleming), pp. 1-36. Oxford: Oxford University Press.

Braga, V. M. M., Hodivala, K. J. and Watt, F. M. (1995). Calcium-induced changes in distribution and solubility of cadherins and their associated cytoplasmic proteins in human keratinocytes. *Cell Adhes. Commun.* **3**, 201-215.

Braga, V. M. M., Najabagheri, N. and Watt, F.M. (1998). Calcium-induced intercellular adhesion of keratinocytes does not involve accumulation of β1 integrins at cell-cell contact sites and does not involve changes in the levels or phosphorylation of the catenins. *Cell Adhes. Commun.* **5**, 137-139.

Braga, V. M. M., Machesky, L. M., Hall, A. and Hotchin, N. A. (1997). The small GTPases Rho and Rac are required for the establishment of cadherin-dependent cell-cell contacts. *J. Cell Biol.* **137**, 1421-1431.

Bubb, M. R., Senderowicz, A. M. J., Sausville, E. A., Duncan, K. L. K. and Korn, E. D. (1994). Jasplakinolide, a cytotoxic natural product, induces actin polymerization and competitively inhibits the binding of phalloidin to F-actin. *J. Biol. Chem.* **269**, 14869-14871.

Calautti, E., Grossi, M., Mammucari, C., Aoyama, Y., Pirro, M., Ono, Y., Li, J. and Dotto, G. P. (2002). Fyn tyrosine kinase is a downstream mediator of Rho/PRK2 function in keratinocyte cell-cell adhesion. *J. Cell Biol.* **156**, 137-148.

Chan, A. Y., Bailly, M., Zebba, N., Segall, J. E. and Condeelis, J. S. (2000). Role of cofilin in epidermal growth factor-stimulated actin polymerization and lamellipod protusion. *J. Cell Biol.* **148**, 531-542.

Clayton, L., Hall, A. and Johnson, M. H. (1999). A role for the Rho-like GTPases in the polarisation of mouse eight-cell blastomeres. *Dev. Biol.* **205**, 322-331.

Collins, J. and Fleming, T. P. (1995). Epithelial differentiation in the mouse pre-implantation embryo: making adhesive cell contacts for the first time. *Trends Biochem. Sci.* **20**, 307-312.

Cramer, L. P. (1999). Role of actin-filament disassembly in lamellipodium protrusion in motile cells revealed using the drug jasplakinolide. *Curr. Biol.* **9**, 1095-1105.

Cramer, L., Briggs, L. and Dawe, H. (2002). Use of fluorescently labelled deoxyribonuclease I to spatially measure G-actin levels in migrating and non-migrating cells. *Cell Mot. Cytoskeleton* **51**, 27-38.

Gloushankova, N. A., Krendel, M. F., Alieva, N. O., Bonder, E. M., Feder, H. H., Vasiliev, J. M. and Gelfand, I. M. (1998). Dynamics of contacts between lamellae of fibroblasts: essential role of the actin cytoskeleton. *Proc. Natl. Acad. Sci. USA* **95**, 4362-4367.

Green, K. J., Geiger, B., Jones, J. C. R., Talian, J. C. and Goldman, R. D. (1987). The relationship between intermediate filaments and microfilaments before and during the formation of desmosomes and adherens-type junctions in mouse epidermal cells. *J. Cell Biol.* **104**, 1389-1402.

Hirai, Y., Nose, A., Kobayashi, S. and Takeichi, M. (1989). Expression and role of E- and P-cadherin adhesion molecules in embryonic histogenesis. I. Lung epithelial morphogenesis. *Development* **105**, 263-270.

Hodivala, K. J. and Watt, F. M. (1994). Evidence that cadherins play a role in the downregulation of integrin expression that occurs during keratinocyte terminal differentiation. *J. Cell Biol.* **124**, 589-600.

Krendel, M. F. and Bonder, E. M. (1999). Analysis of actin filament bundle dynamics during contact formation in live epithelial cells. *Cell Motil. Cytoskeleton* **43**, 296-309.

Krendel, M., Gloushankova, N. A., Bonder, E. M., Feder, H. H., Vasiliev, J. M. and Gelfand, I. M. (1999). Myosin-dependent contractile activity of the actin cytoskeleton modulates the spatial organization of cell-cell contacts in cultured epitheliocytes. *Proc. Natl. Acad. Sci. USA* **96**, 9666-9670.

Littlefield, R., Almenar-Queralt, A. and Fowler, V. M. (2001). Actin dynamics at pointed ends regulates thin filament length in striated muscle. *Nat. Cell Biol.* **3**, 544-551.

Mandato, C. A. and Bement, W. M. (2001). Contraction and polymerization cooperate to assemble and close actomyosin rings around Xenopus oocyte wounds. *J. Cell Biol.* **154**, 785-798.

McNeill, H., Ryan, T. A., Smith, S. J. and Nelson, J. W. (1993). Spatial and temporal dissection of immediate and early events following cadherin-mediated epithelial cell adhesion. *J. Cell Biol.* **120**, 1217-1226.

Nelson, W. J. (2003). Adaptation of core mechanisms to generate cell polarity. *Nature* **422**, 766-774.

Noren, N. K., Niessen, C. M., Gumbiner, B. M. and Burridge, K. (2001). Cadherin engagement regulates Rho family GTPases. *J. Biol. Chem.* **276**, 33305-33308.

Owaribe, K., Kodama, R. and Eguchi, G. (1981). Demonstration of contractility of circumferential actin bundles and its morphogenetic significance in pigmented epithelium in vitro and in vivo. *J. Cell Biol.* **90**, 507-514.

Philip, N. J. and Nachmias, V. T. (1985). Components of the cytoskeleton in the retinal pigmented epithelium of the chick. *J. Cell Biol.* **101**, 358-362.

Pollard, T. D., Blanchoin, L. and Mullins, R. D. (2000). Molecular mechanisms controlling actin filament dynamics in non muscle cells. *Annu. Rev. Biophys. Biomol. Struct.* **29**, 545-576.

Ridley, A. J., Schwartz, M. A., Burridge, K., Firtel, R. A., Ginsberg, M. H., Borisy, G., Parsons, J. T. and Horwitz, A. R. (2003). Cell migration: integrating signals from front to back. *Science* **302**, 1704-1709.

Sahai, E. and Marshall, C. J. (2002). ROCK and Dia have opposing effects on adherens junctions downstream of Rho. *Nat. Cell Biol.* **4**, 408-415.

Sanger, J. W., Sanger, J. M. and Jockusch, B. M. (1983). Differences in the stress fibers between fibroblasts and epithelial cells. *J. Cell Biol.* **96**, 961-969.

Sharpe, G. R., Fisher, C., Gillespie, J. I. and Greenwell, J. R. (1993). Growth and differentiation stimuli induce different and distinct increases in intracellular free calcium in human keratinocytes. *Arch. Dermatol. Res.* **284**, 445-450.

Shimoyama, Y., Yoshida, T., Terada, M., Shimosato, Y., Abe, O. and Hirohashi, S. (1989). Molecular cloning of a human Ca2+-dependent cell-cell adhesion molecule homologous to mouse placental cadherin: its low expression in human placental tissues. *J. Cell Biol.* **109**, 1787-1794.

Stoffler, H. E., Honnert, U., Bauer, C. A., Hofer, D., Schwarz, H., Muller, R. T., Dreckhahn, D. and Bahler, M. (1998). Targeting of the myosin-I to intercellular adherens type junctions induced by dominant active Cdc42 in Hela cells. *J. Cell Sci.* **111**, 2779-2788.

Straight, A. F., Cheung, A., Limouze, J., Chen, I., Westwood, N. J., Sellers, J. R. and Mitchison, T. J. (2003). Dissecting temporal and spatial control of cytokinesis with a myosin II inhibitor. *Science* **299**, 1743-1747.

Theriot, J. A. and Mitchison, T. J. (1991). Actin microfilament dynamics in locomoting cells. *Nature* **352**, 126-131.

Vaezi, A., Bauer, C., Vasioukhin, V. and Fuchs, E. (2002). Actin cable dynamics and Rho/Rock orchestrate a polarized cytoskeletal architecture in the early steps of assembling a stratified epithelium. *Dev. Cell* **3**, 367-381.

Vasioukhin, V., Bauer, C., Yin, M. and Fuchs, E. (2000). Directed actin polymerization is the driving force for epithelial cell-cell adhesion. *Cell* **100**, 209-219.

Wissmann, A., Ingles, J. and Mains, P. E. (1999). The *Caenorhabditis elegans* mel-11 myosin phosphatase regulatory subunit affects tissue contraction in the somatic gonad and the embryonic epidermis and genetically interacts with the Rac signalling pathway. *Dev. Biol.* **209**, 111-127.

Wozniak, M. A., Desai, R., Solski, P. A., Der, C. J. and Keely, P. J. (2003). ROCK-generated contractility regulates breast epithelial cell differentiation in response to the physical properties of a three-dimensional collagen matrix. *J. Cell Biol.* **163**, 583-595.

Yap, A. S., Brieher, W. M. and Gumbiner, B. M. (1997). Molecular and functional analysis of cadherin-based adherens junctions. *Annu. Rev. Cell Dev. Biol.* **13**, 119-146.

Yonemura, S., Itoh, M., Nagafuchi, A. and Tsukita, S. (1995). Cell-to-cell adherens junction formation and actin filament organization: similarities and differences between non-polarized fibroblasts and polarized epithelial cells. *J. Cell Sci.* **108**, 127-142.

Zamansky, G. B., Nguyen, U. and Chou, I.-N. (1991). An immunofluorescence study of the calcium-induced coordinated reorganization of microfilaments, keratin intermediate filaments, and microtubules in cultured human epidermal keratinocytes. *J. Inv. Dermatol.* **97**, 985-994.

Zhong, C., Kinch, M. S. and Burridge, K. (1997). Rho-stimulated contractily contributes to the fibroblastic phenotype of Ras-transformed epithelial cells. *Mol. Biol. Cell* **8**, 2329-2344.